PARAMETERIZATION OF THE FAIR WEATHER EKMAN LAYER

J. F. PRICE
Woods Hole Oceanographic Institution
Woods Hole, Massachusetts USA

Abstract

Most models of the upper ocean Ekman layer require a parameterization of turbulent mixing. Two very simple forms of parameterization are considered here and compared with fair weather data sets. A steady classical diffusion model is found to give reasonably good simulations with familiar values of diffusivity. However, the solutions show a systematic error in current direction that arises, apparently, from a non-parallel relation between shear and stress in the observed profiles.

Inspection of these and other data suggests that the transient, surface-trapped stratification associated with the diurnal cycle is likely to be important in fair weather conditions. The process of diurnal cycling can be treated in a layered model to yield a closed solution for Ekman layer currents. This solution has some of the characteristics of a useful parameterization for use in an OGCM, though it covers only a part of the relevant parameter range.

1. The Upper Ocean Ekman Layer

The upper ocean Ekman layer presents two significant problems – to observe and describe the currents due to an imposed wind stress, and to develop accurate and physically consistent models of wind-driven currents that can be applied over a wide range of conditions. In this note we examine some recent upper ocean observations, and consider some issues of Ekman layer parameterization. Readers looking for a broader perspective on the Ekman layer should see Kraus and Businger (1994), and for a review of upper ocean models, Nurser (1996).

The essential dynamics of wind-driven currents were identified almost 100 years ago in Walfrid Ekman's (1905) landmark analysis. From some very limited observations of wind-driven ice motion, Ekman realized that (1) the Coriolis acceleration due to earth's rotation was crucially important for wind-driven currents, as was already understood well for geostrophic currents, and (2) wind stress must be absorbed over a surface boundary layer having a thickness of order several tens of meters. The latter implies that wind stress must be transmitted downward from the surface as a turbulent momentum flux, $\boldsymbol{\tau}$, that cannot be observed directly in most open ocean conditions (see McPhee and Martinson, 1994, for an example of turbulent stress measured under ice). Away from boundaries and other strong ocean currents, the momentum balance of a steady wind-driven current is expected to be largely between the Coriolis and wind stress accelerations,

$$f\boldsymbol{V}\exp(i\frac{\pi}{2}) = \frac{1}{\rho}\,\frac{\partial\boldsymbol{\tau}}{\partial z}, \tag{1}$$

where f is the Coriolis parameter, ρ is the nominal density of sea water, $\boldsymbol{V}$ is the steady or time-averaged current (with stress averaged the same way and bold symbols denoting complex variables). Boundary conditions are presumed known on $\boldsymbol{\tau}$: that it equals the given wind stress at the surface, and that it vanishes along with the current at the depth of semi-permanent stratification, $z = z_r$, also presumed to be given from observations. The crux of the theoretical half of the Ekman layer problem is to calculate the stress within the water column above z_r so that the current profile $\boldsymbol{V}(z)$ can also be calculated. This is a classical problem in turbulent parameterization that has been studied intensively since Ekman (1905) and yet is still unsolved in important ways today.

The observational half of the Ekman layer problem requires accurate current measurements near the sea surface, which has been possible only since about 1980 (Weller and Davis, 1980; Weller, 1981). Two recent data sets (Price *et al.*, 1987, and Chereskin, 1995; Figure 1) provide what appears to be a reliable view of the upper ocean Ekman layer in fair weather, subtropical conditions. The current profiles have a spiral shape in which the current speed decays with depth as the current vector rotates to the right — this is very similar to a classical Ekman spiral.

This note addresses two specific questions: **What processes set the thickness and the shape of these current profiles?** and, **How can the relevant processes be parameterized within simple models?** There is now a full spectrum of upper ocean models that are relevant to the Ekman layer problem, and it may be helpful to point out where the present 'simple' models will fall, and also to clarify a second way in which the term 'parameterization' will be used. At the greatest resolution are numerical

TABLE 1. Some relevant external variables and depth scales estimated from the current profiles. Q is the average daily maximum heat flux. Current e-folding is the e-folding scale of the current speed estimated by fitting an exponential to the speed profile. Current turning is the depth over which the current turns through one radian, estimated by fitting a straight line to the direction profile.

Data set	f (10^{-5}s^{-1})	τ (Pa)	Q (W m^{-2})	Current e-folding (m)	Current turning (m)
LOTUS3	8.36	0.07	630	10	18
EBC	8.77	0.09	570	16	66

turbulence models that compute explicitly nearly all of the stress-carrying part of the turbulence and require parameterization of only the smallest, dissipative scales (McWilliams *et al.*, 1997). These models are enormously powerful research tools, but they are also very demanding computationally and for that reason they generally can not be used to represent, or parameterize, upper ocean processes within OGCMs. At a step down in resolution, there is a wide range of intermediate numerical models that have sufficient temporal and spatial resolution to be run with synoptic surface fluxes and that can simulate the evolution of the seasonal and diurnal thermocline (Mellor and Durbin, 1975; Price *et al.*, 1986; Large *et al.*, 1994; Large, 1998, discusses some of these models). These intermediate models parameterize nearly all aspects of turbulence, and they are generally affordable for use as the upper ocean component of three-dimensional circulation models. At still another major step down in resolution are the kind of truly simple models that are emphasized here, a familiar example being Ekman's (1905) classical diffusion model. These models too must parameterize all aspects of turbulence, and in addition they can accept only limited surface flux information, e.g., time-averaged wind stress in place of the time series of wind stress that was possible at the intermediate level. Hence their turbulence parameterizations may be very different from that used at the previous model level. These models make almost no computational demand, and in some limits they can be solved explicitly. These most-reduced models and their solutions may be suitable as upper ocean parameterizations in some circumstances (e.g., when only climatological surface flux data is available) but their intrinsic value is that they may help us reach a deeper understanding of Ekman layer phenomenon.

The two questions noted above could be taken in either order, but given the obvious similarity of the observed spirals to classical Ekman spirals we begin with the turbulent parameterization question and the classical diffusion theory.

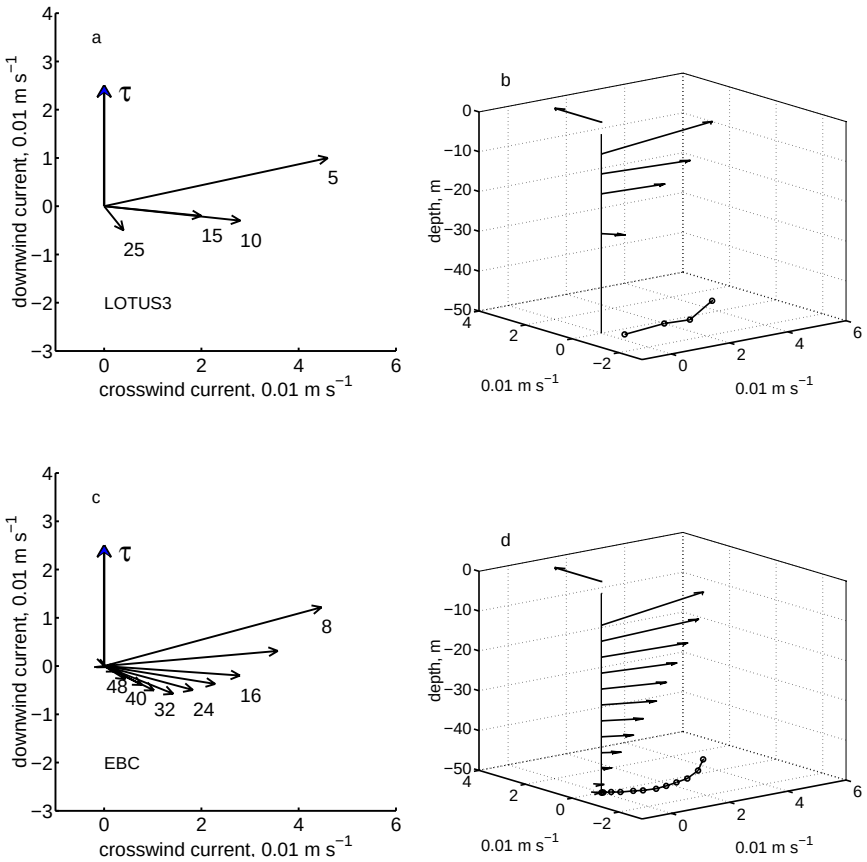

Figure 1. Hodographs and three-dimensional profiles of time-averaged upper ocean currents and wind stress. (a, b) Observations from LOTUS3 in the western Sagrasso Sea (after Price *et al.*, 1987). (c, d) Observations from the Eastern Boundary Current Experiment (after Chereskin, 1995, hereafter, EBC). The LOTUS3 data were collected over the summer half of the year at 35N in the western Sargasso Sea (Table 1). The EBC mooring was at 37N in the eastern North Pacific also during the summer. The reference frames have been rotated so that wind stress points northward in hodographs (the τ vector indicates direction only) and the depth in meters is written just below the tip of the current vectors. Note that these two current profiles are very similar, which is reassuring since the external conditions were also very similar (Table 1).

2. Diffusion Theory

As a first model of the turbulent momentum flux, Ekman adopted Boussinesq's hypothesis of ca. 1870 that a turbulent stress might be treated by analogy with a laminar (molecular) stress,

$$\boldsymbol{\tau}/\rho = K\frac{\partial \boldsymbol{V}}{\partial z}, \tag{2}$$

where K, the eddy diffusivity, represents the stirring effects of turbulence acting upon the vertical shear of the time-mean (or steady) wind-driven current, $\boldsymbol{V}$ (a concise review of the eddy diffusivity concept is in Frisch, 1995).

This parameterization places nearly the entire burden of the problem upon the specification of K, and indeed it is not too strong to say that it turns the Ekman layer problem into the task of finding a suitable K. This would be an inspired step if it turned out that K was in any sense simpler than the current profile itself, i.e., if K had simpler depth-dependence or reduced parameter dependence. Experimental and theoretical efforts to determine K in this and other contexts have formed a major research program on geophysical turbulence, though it is not evident that there has been a convergence on any particular form (Pollard, 1975; Huang, 1979). This vagueness serves to inoculate the classical diffusion theory against critical test, since any particular version of K will appear to be no more than a strawman.

2.1. THE LAMINAR DIFFUSION MODEL

The classical 'laminar' diffusion model, CLDM, presumes that K is constant with depth and yields the Ekman spiral, which we have already noted is visually similar to the observed spirals. The CLDM can be solved given a steady wind stress, taken 'north' (or imaginary), and boundary conditions as noted above (with $z_r = -H$). Denoting the diffusive length scale within the upper ocean by

$$D_K = \sqrt{2K/f}, \tag{3}$$

and normalizing depth by H,

$$z' = z/H,$$

the solution is (Gonella, 1971),

$$\boldsymbol{V}(z) = U_n\frac{\alpha}{\sqrt{2}}[a\exp(-(1+i)z'\alpha) + b\exp((1+i)z'\alpha)], \tag{4}$$

where

$$\begin{aligned} a &= \exp(i\pi/4)(\exp(2\alpha) - \exp(i2\alpha))/c, \\ b &= \exp(i\pi/4)(\exp(-i2\alpha) - \exp(-2\alpha))/c, \\ c &= \cosh(2\alpha) - \cos(2\alpha). \end{aligned}$$

The scale

$$U_n = \frac{U_*^2}{Hf}$$

is called the 'neutral' velocity scale, and the only non-dimensional parameter is

$$\alpha = H/D_K.$$

This solution simplifies considerably in two important limits. In the limit $\alpha << 1$, say because K is very large, then the solution is just

$$\boldsymbol{V}(z) = U_n \tag{5}$$

in the depth range $-H < z < 0$, and vanishing below. The Ekman layer current is then depth-independent (i.e., slab-like) and flows at right angles to the wind stress. In the other limit, when $\alpha >> 1$, say because K is small, then this solution reduces to the classical Ekman spiral for infinite water depth,

$$\boldsymbol{V}(z) = U_n \alpha \exp(z'\alpha) \exp(iz'\alpha)(1+i).$$

The surface current is a well-known result

$$\boldsymbol{V}(0) = \frac{U_*^2}{\sqrt{fK}} \exp(i\frac{\pi}{4}). \tag{6}$$

This CLDM solution is parametric in K, which must be specified for any practical use. In the absence of an accepted form, the best fit K, K_b, was found by minimizing the root mean square vector misfit between the CLDM solution (4) and the observed currents (Table 2). In both cases there was a distinct minimum of the misfit, and thus a well defined K_b and a corresponding solution that looks fairly good (Figure 2a,b). These estimated K_b are well within the (large) range inferred from other analyses (Pollard, 1975). In the EBC case the CLDM solution had an rms misfit of only about 0.007 m s^{-1}, and accounted for 89% of the variance of the observed currents. A solution this accurate would suffice for many practical purposes, assuming that one could predict K. These two cases are nearly identical and give little clue to K dependence, but they are not far from the neutral, turbulent Ekman layer scale, $h_E = c_1 U_*/f$, where h_E is the e-folding depth scale (Table 1) from which a diffusivity can be inferred. In these cases $c_1 = 0.1$, while the nominal value is $c_1 = 0.25$ (Coleman *et al.*, 1990; McPhee and Martinson, 1994).

On closer inspection, there is seen to be an error in the current direction and in the shape of the spiral. The error is small near the surface and increases with depth to roughly 45 degrees. For many purposes this directional error might not be significant since it occurs mainly at depth. Such

TABLE 2. Statistical measures of the CLDM and SEL4 solutions (the SEL4 is developed in Section 3). The best fit diffusivities for the former (K_b) and the rms vector error (Misfit) and the percent variance accounted for (PV) are shown for each model.

Data set	rms V	CLDM solution			SEL4 solution	
		K_b (10^{-4} m^2 s^{-1})	Misfit (m s^{-1})	PV	Misfit (m s^{-1})	PV
LOTUS3	0.026	100 ± 20	0.011	83	0.008	90
EBC	0.021	175 ± 25	0.007	89	0.005	94

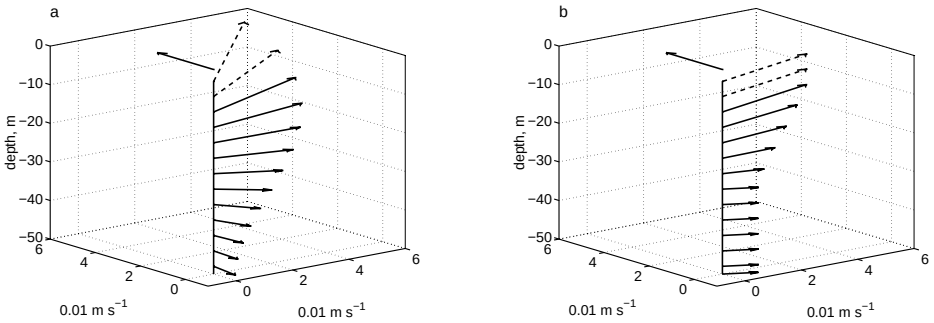

Figure 2. Three-dimensional profiles of the horizontal current computed by the best fit CLDM solution (a), and by the SEL4 solution (b). External parameters were those of the EBC data set (Table 1) and the solution is plotted at the nominal 4 m depth interval of the EBC observations; dashed current vectors at $z = 0$ and -4 m are shallower than the available observations (cf. Figure 1d).

a small error would probably not be considered a reliable indicator if it occurred in only one example. However, a very similar directional error is evident in the LOTUS3 case as well, and a closely related phenomenon is the reported mismatch of diffusivity estimated from current direction and speed (the former being larger, Weller, 1981; Chereskin, 1995).

2.2. A DIAGNOSED DIFFUSIVITY

An unconstrained diffusivity can be diagnosed from the observed current profile. The EBC data is best suited for this purpose since it has very good vertical resolution. The stress profile was estimated by integrating the steady momentum balance (1) upward from the reference depth $z_r = -H$, where the wind-driven current and stress were presumed to vanish (Figure

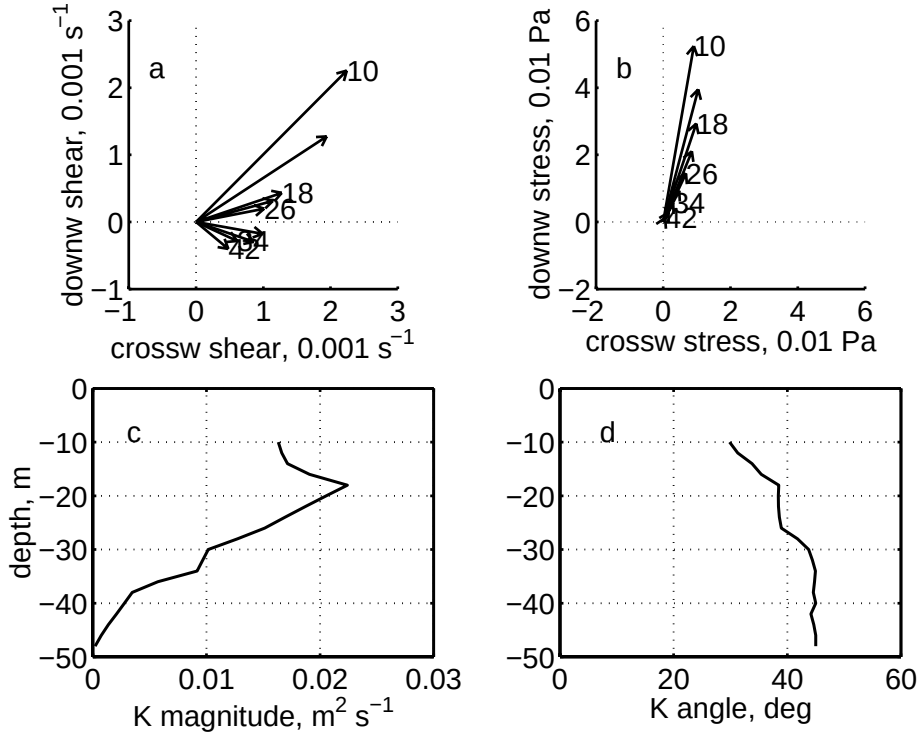

Figure 3. (a) Shear profile estimated from the EBC current profile. (b) Stress profile inferred from the EBC current profile and assuming a steady momentum balance throughout the water column. (c) The amplitude of the complex diffusivity estimated from (a) and (b). (d) The angle of the complex-valued diffusivity. Angles greater than zero indicate that the stress vector at a given depth is to the left of the corresponding shear vector, as can be seen comparing (a) and (b).

3, and see also Chereskin, 1995). The resulting stress profile extrapolates to approximately the wind-derived estimate of stress at the sea surface, as expected from Chereskin's (1995) analysis of the transport. The vertical shear is readily computed, and the stress and shear may be compared in hodographs (Figure 3a and b). The shear and the stress are evidently not parallel; the stress vector points more nearly downwind than does the shear vector by roughly 40 degrees, but depending upon depth. This non-parallel relation between stress and shear is the root of the direction error made by the CLDM. A non-parallel shear/stress relation has been found also in numerical calculations of turbulent Ekman layers (Coleman *et al.*, 1990) where it evidently arises from the large eddy structure of Ekman layer turbulence, and in the analysis of surface drifter data (Krauss, 1993).

The classical diffusion model could accommodate this non-parallel rela-

tion between stress and shear by admitting a complex-valued $K(z)$, (Figure 3c and d). But this complex K is no simpler than the current profile itself, and the prospects of finding or developing a universal form of K are not brightened (and indeed Rossby similarity theory, e.g., Kraus and Businger, 1994, seems just as apt). While diffusion theory offers ample room for development, it may be useful to consider what might have been overlooked at the starting point, Eq (2).

3. A Model of the Stratified Ekman Layer

Under the fair weather conditions that held during both observation periods, the upper ocean density profile is often stratified and remixed on a diurnal cycle. This is accompanied by corresponding large variations in the thickness of the turbulent surface layer and in the current profile (Brainerd and Gregg, 1993; Price *et al.*, 1986). The effects of this diurnal variability can be assessed within a layered model that leads to a closed solution for the time-averaged, wind-driven current.

3.1. A LAYERED MODEL

The mixed layer depth is presumed to vary with a top-hat time-dependence over the course of a day, with the shallow, daytime mixed layer depth being the trapping depth defined by Price *et al.* (1986; hereafter, PWP),

$$D_Q = \frac{U_*^2 P_\tau}{\sqrt{Q_* P_Q / 2.}}, \tag{7}$$

where $P_\tau = (1/f)\sqrt{2 - 2\cos(f P_Q/2)}$, P_Q is the interval during which the surface heat flux is warming, and $Q_* = g\gamma Q/\rho C_p$, with Q the amplitude of the daily maximum heat flux, γ the thermal expansion coefficient and C_p the heat capacity of sea water. The idea behind D_Q is that the thickness of the diurnal warmed layer is set by a Richardson number condition based upon the temperature difference (a proxy for the density difference) and the vertical shear of the wind-driven current (the diurnal jet). The time-averaged two layer wind-driven current can then be computed from the time-dependent momentum balances (details in Price and Sundermeyer, 1998). Within the upper layer 1, $z \geq -D_Q$,

$$\boldsymbol{V}_1 = U_n \left[1 + (\alpha - 1)\sqrt{\Psi_r^2 + \Psi_i^2}\exp(i\theta) \right], \tag{8}$$

while in the lower layer 2, $-H < z < -D_Q$,

$$\boldsymbol{V}_2 = U_n \left[1 - \sqrt{\Psi_r^2 + \Psi_i^2}\exp(i\theta) \right]. \tag{9}$$

The scale $U_n = \frac{U_*^2}{fH}$, exactly as before for the CLDM solution, and in this context,

$$\alpha = H/D_Q.$$

This is analogous to the ratio H/D_K of the CLDM, but note that this α depends only upon external variables. The angle

$$\theta = \mathrm{atan}(\frac{\Psi_i}{\Psi_r}),$$

where the $\Psi_{r,i}$ are functions of the phases, fP_Q and fP_{24}, which do not have a counterpart in the CLDM,

$$\Psi_r = \frac{fP_Q - \sin(fP_Q)}{fP_{24}}, \quad \text{and} \quad \Psi_i = \frac{1 - \cos(fP_Q)}{fP_{24}},$$

where P_{24} is the length of a day.

3.2. EMBELLISHMENTS AND A CONSISTENCY CHECK

These are the essential results for the layered model, but if the full profile of the Ekman layer current is required then the profile structure must be considered further. The two layer model taken literally indicates a velocity jump between the layers. There is, of course, no such velocity jump found in the ocean, nor in any highly resolved upper ocean model (Figure 4). To simulate a continuous profile a third, intermediate layer of thickness D_Q is therefore inserted into the solution on what is admittedly an *ad hoc* basis. Velocity in this intermediate layer is computed by a linear interpolation in the depth range $-1.5D_Q < z < -0.5D_Q$. Another velocity jump occurs at the bottom of layer 2, at $z = -H$. At subtropical or higher latitudes this velocity jump will usually be quite small. However, at lower latitudes the deep Ekman layer currents can be fairly large, O(0.1 m s^{-1}), and cause significant mixing. To simulate this feature a fourth (and final) layer has been added, whose thickness is set by a critical gradient Richardson number condition. Thus the velocity profile may show up to four distinct layers, two vertically uniform and two vertically sheared, and the solution is termed SEL4 (four layer stratified Ekman layer).

The SEL4 solution is free from adjustable parameters, and can be readily evaluated given the surface fluxes and H as before, plus the daily maximum surface heating and the duration of heating. The SEL4 profiles look reasonably good (compare Figure 2b with 1d) and the percent variance accounted for is $\geq 90\%$, or slightly better than the CLDM solution (Table 2).

The most obvious error is at depth (Figure 2), where both the CLDM and SEL4 solutions overestimate the speed of the observed current. This can

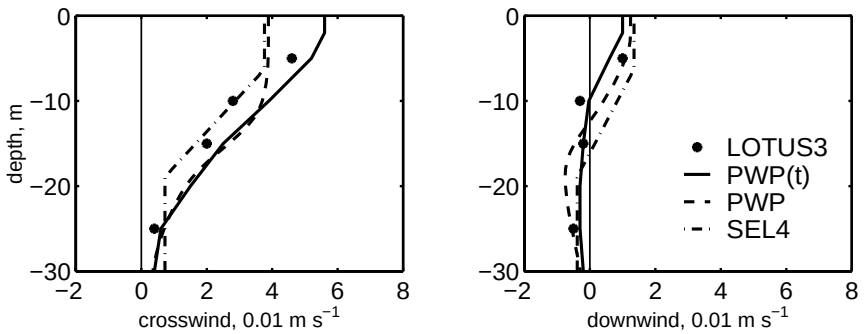

Figure 4. Crosswind and downwind Ekman layer currents from the LOTUS3 data set (discrete points) and as computed by the PWP numerical model run with the hourly surface fluxes (solid line, PWP(t), after Price *et al.*, 1987), by the PWP numerical model run with time-averaged fluxes (dash-dot line, PWP) and by the SEL4 solution (dashed line, SEL4). This comparison serves to check several approximations made during the development of the SEL4 solution and in particular the greatly simplified time-dependence of mixed layer depth (SEL4 compared with PWP). It also shows that the use of time-averaged fluxes in place of hourly fluxes does not introduce large errors (PWP (and SEL4) compared with PWP(t)).

be attributed at least partly to the assumption that the depth of semipermanent stratification, H, was constant. Within the LOTUS3 data set, the advection by internal wave motions alone was about 15 m peak-peak at 50 m depth. This would have a significant smearing effect on the mean current (Davis *et al.*, 1981) that is not represented in the models, and that greatly exceeds the layer four thickness of the SEL4 model.

3.3. PARAMETER DEPENDENCE OF THE SURFACE CURRENT

The parameter dependence of the surface current reveals some of the character of the SEL4 solution and can be compared directly with that of the CLDM solution. First, if D_Q approaches H, say because heating is negligible or wind stress is strong, then diurnal cycling is of no consequence. This arises when

$$\frac{Q_* P_Q H^2}{U_*^4 P_\tau^2} \leq 1, \tag{10}$$

which is the condition that defines weak heating. In that case the surface current goes as the neutral limit,

$$\boldsymbol{V}_1 = U_n, \tag{11}$$

exactly as does the CLDM in the limit of large K, Eq (5). This is not an interesting result for this model, and neither is it likely to be a realistic

solution for a neutral Ekman layer. At the other extreme when $D_Q \ll H$, analogous to the CLDM limit of very small K, Eq (6), the surface current

$$\boldsymbol{V}_1 = U_h \exp(i\theta), \tag{12}$$

where

$$U_h = \frac{\sqrt{Q_* P_Q/2}}{f P_\tau} \sqrt{\Psi_r^2 + \Psi_i^2}$$

is termed the 'heating' scale. This is an interesting result in as much as U_h is independent of the stress. The EBC and LOTUS3 cases approach this limit and $U_h \approx 0.04$ m s^{-1}, which is consistent with the shallowest measured speeds (Figure 1). Most conditions, i.e., most days and most places, will fall between these two extremes and the surface Ekman current computed by SEL4 will depend upon both H and D_Q. The stress-dependence of the surface current will then be intermediate as well.

The direction of the surface current varies with latitude and heating, but typically the surface current is well to the right of the wind ($f \geq 0$) and the current profiles are 'flat' compared to a classical Ekman spiral. In the large α limit, the surface current direction (for EBC or LOTUS3 latitude and P_Q =13 hrs) is $\theta = \text{atan}(\Psi_i/\Psi_r) = 15$ degrees, or 75 degrees to the right of the wind stress (Figure 1). In this regard the SEL4 solutions tend to be a little more realistic than are the CLDM solutions.

4. Remarks

A checklist of desirable qualities of a theory, model, or parameterization might include accuracy, consistency, simplicity, scope, and fruitfulness (Kuhn, 1977), to which we add falsifiability. Simplicity is clearly a virtue of the models considered here, and fruitfulness is an issue for the future.

Accuracy compared to some absolute standard, here taken to be the LOTUS3 and EBC observations. Both the SEL4 and the CLDM solutions exhibit reasonably good accuracy (measured by rms misfit and compared to uncertainties in the data themselves), though CLDM had the advantage of an adjustable parameter.

Consistency with an accepted or more fundamental theory, here measured only for SEL4 and only by comparison with the PWP numerical model results, which would not count as an accepted standard. This comparison did serve to test the conjecture that surface fluxes could be represented by their average values, and found to be valid at least for the LOTUS3 case where wind stress was especially variable. Comparisons with much more sophisticated turbulence-resolving models (as in McWilliams *et al.*, 1997) could show whether the observed flat spiral shape could arise even in the absence of diurnal cycling.

Scope sufficient for the required applications and ideally beyond the domain of construction. If the task were to estimate Ekman layer currents at an arbitrary location and season, then the SEL4 solution would not be a good candidate, since it is applicable only to fair weather conditions. The range of application is at least known, being defined by Eq (10). It is clear that the phenomena included in SEL4 are only a subset of possible Ekman layer dynamics and that more comprehensive models, not so constrained in their formulation, are needed for practical applications.

Falsifiability in the face of conflicting, relevant observations. The greatest virtue of SEL4 when compared with classical diffusion models is that it is closed, and without adjustable parameters. The SEL4 solution can be evaluated unambiguously, and if it truly fails, then it can be declared truly dead in a way that the classical diffusion models probably never can be.

5. Access and Acknowledgements

The models described here are available from J. Price (jprice@whoi.edu). At the time of this writing, they can also be retrieved from the anonymous ftp site 128.128.29.54, cd pub/ekman. Most of this note is taken from Price and Sundermeyer (1998), which is also accessible from the same directory.

JFP's research on upper ocean dynamics has been supported by the US Office of Naval Research under contract N00014-95-1-0105.

References

Brainerd, K. E. and M. C. Gregg (1993) Diurnal restratification and turbulence in the oceanic surface mixed layer 1. Observations. *Journal of Geophysical Research*, **98**, 22645–22656.

Chereskin, T. K. (1995) Direct evidence for an Ekman balance in the California Current. *Journal of Geophysical Research*, **100**, 18261–18269.

Coleman, G. N., J. H. Ferziger and P. R. Spalart (1990) A numerical study of the turbulent Ekman layer. *Journal of Fluid Mechanics*, **213**, 313–348.

Davis, R. E., R DeSzoeke, D. Halpern and P. Niiler (1981) Variability in the upper ocean during MILE, I: The heat and momentum balances. *Deep-Sea Research*, **28**, 1427–1451.

Ekman, V. W. (1905) On the influence of the earth's rotation on ocean currents. *Arch. Math. Astron. Phys.*, **2**, 1–52.

Frisch, U. (1995) *Turbulence*. Cambridge University Press, Cambridge, England.

Gonella, J. (1971) A local study of inertial oscillations in the upper layers of the ocean. *Deep-Sea Research*, **18**, 775–788.

Huang, N. E. (1979) On surface drift currents in the ocean. *Journal of Fluid Mechanics*, **91**, 191–208.

Kraus, E. B., and J. A. Businger (1994) *Atmosphere–Ocean Interaction*. 2nd Ed. Oxford University Press, New York. 362 pp.

Krauss, W. (1993) Ekman drift in homogeneous waters. *Journal of Geophysical Research*, **98**(C11), 20187–20209.

Kuhn, T. S. (1977) Objectivity, value judgment and theory choice. In *The Essential Tension*. The University of Chicago Press. Chicago.

Large, W. G., J. C. McWilliams and S. C. Doney (1994) Oceanic vertical mixing: A review and a model with nonlocal boundary layer parameterization. *Review of Geophysics*, **32**, 363–403.

Large, W. G. (1998) Modeling and parameterizing ocean planetary boundary layers. In *Ocean Modeling and Parameterization*, E.P. Chassignet and J. Verron (Eds.), Kluwer Academic Publishers, 81–121.

McPhee, M. G. and D. G. Martinson (1994) Turbulent mixing under drifting pack ice in the Weddell Sea. *Science*, **263**, 218–221.

McWilliams, J. C., P. S. Sullivan and C.-H. Moeng (1997) Langmuir turbulence in the ocean. *Journal of Fluid Mechanics*, **334**, 1–30.

Mellor, G. L. and P. A. Durbin (1975) The structure and dynamics of the ocean surface mixed layer. *Journal of Physical Oceanography*, **5**, 718–728.

Nurser, A. J. G. (1996) A review of models and observations of the oceanic mixed layer. Internal Document 14, Southampton Oceanographic Center. Southampton, England.

Pollard, R. T. (1975) Observations and models of the structure of the upper ocean. In: *Modelling and Prediction of the Upper Layers of the Ocean*, E. B. Kraus, Editor, Pergamon Press, Oxford, England.

Price, J. F., R. A. Weller and R. Pinkel (1986) Diurnal cycling: Observations and models of the upper ocean response to heating, cooling and wind mixing. *Journal of Geophysical Research*, **91**, 8411–8427.

Price, J. F., R. A. Weller and R. R. Schudlich (1987) Wind-driven ocean currents and Ekman transport. *Science*, **238**, 1534–1538.

Price, J. F. and M. A. Sundermeyer (1998) Stratified Ekman layers. *Journal of Geophysical Research*, submitted.

Weller, R. A. (1981) Observations of the velocity response to wind forcing in the upper ocean. *Journal of Geophysical Research*, **86**, 1969–1977.

Weller, R. A., and R. E. Davis (1980) A vector measuring current meter. *Deep-Sea Res.*, **27**, 565–582.